BAFFLE: A 3D printable device for macroscopic quantification of fluorescent bacteria in space and time

Carles Tardío Pi[1], Daniela Reyes-González[2], Andrea Fernández-Duque[1], Ayari Fuentes-Hernández[2], Fernando Santos-Escobar[1], and Rafael Peña-Miller[1,*]

[1] *Laboratorio de Biología de Sistemas, Centro de Ciencias Genómicas, Universidad Nacional Autónoma de México, 62210, Cuernavaca, Mexico.*

[2] *Laboratorio de Biología Sintética, Centro de Ciencias Genómicas, Universidad Nacional Autónoma de México, 62210, Cuernavaca, Mexico.*

[*] *Corresponding author: rpm@ccg.unam.mx*

Abstract

Despite the ubiquity and importance of microbial communities, understanding the population dynamics of mixed cultures in structured environments remains a fundamental problem in microbial ecology. Identifying bacterial strains within a complex microbial community represents a challenging technical problem. We describe a low-cost optomechanical device designed to acquire multi-channel time-lapse images of bacterial colonies growing in agar plates. This device uses a system of addressable LEDs and fluorescence filters to estimate the spatio-temporal distribution of different fluorescently-tagged cells from time-lapse images obtained using a standard DSLR camera with a macro lens. We demonstrate the potential of this device with a range of applications from experimental microbiology.

Metadata Overview

Main design files: https://github.com/ccg-esb-lab/baffle
DOI archive: https://doi.org/10.5281/zenodo.6960207
Building instructions: https://www.penamiller.com/lab/baffle
Scripts to produce figures: https://github.com/ccg-esb-lab/BAFFLE/tree/master/macros
Raw data needed to produce figures: https://github.com/ccg-esb-lab/BAFFLE/tree/master/data
Target group: school or academic staff, NGOs and scientific staff.
Skills required for building the device: 3D printing – intermediate; mechanical assembly – intermediate; electrical assembly – intermediate;
Replication: No builds known to the authors so far.

Keywords

microbiology; fluorescence imaging; macro photography

Introduction

An extensive collection of low-cost open-source imaging systems is nowadays available for microscopic image capture [38, 28, 29, 42]. These devices are developed following an open philosophy, and therefore code and hardware design are openly shared so that a broader range of researchers can build, modify, and improve existing projects [9]. However, only a narrow range of such devices is oriented towards

[*] BAFFLE acronym stands for "Bionic Apparatus For Fluorescent Light Estimation" and it was coined in relation to the first version of the device encased inside a wooden speaker box.

the acquisition of systematic spatio-temporal information within the macroscopic cellular scale between millimeter to centimeter range [12], an arena in which bacterial spatial structure manifests itself and becomes relevant due, for example, to biofilm structure formation during colony growth [19].

In this manuscript, we detail the construction, assembly, and operational guide of a tunable low-cost and open-source programmable imaging system established for *in vivo* multi-fluorescence macro-photography capture of Petri dish cultures under controlled environmental conditions. As illustrated in Figure 1, the design is modular with a temperature and humidity controlled incubator chamber combined with a customizable mechanical switching 4 fluorescent exciter and filter wheel coupled to a macro-camera with controlled focus through a z-axis step motor. Moreover, the system can capture high quality dark and bright field macro-images using a led flash-lighting system mounted inside the incubator chamber compartment, which can modulate R, G, B, and alpha light parameters and its incidence angle to achieve different light and shadow characteristics helpful in revealing 3D bacterial structure through image stacking techniques. The device is controlled through a dedicated GUI browser application, which allows the selection of the desired optical, camera, light, temperature and humidity, and time-lapse sequence configurations and settings.

We report and demonstrate the usefulness and robustness of the system with a range of applications where a combination of image acquisition and analysis can be used to obtain quantitative data on the distribution of fluorescently tagged bacteria during surface colonization. We will show that, by estimating the frequency of different strains in time and space, we can estimate fitness of each strain and obtain quantitative information about the ecological interactions that result from multiple microbial subpopulations interacting through the environment.

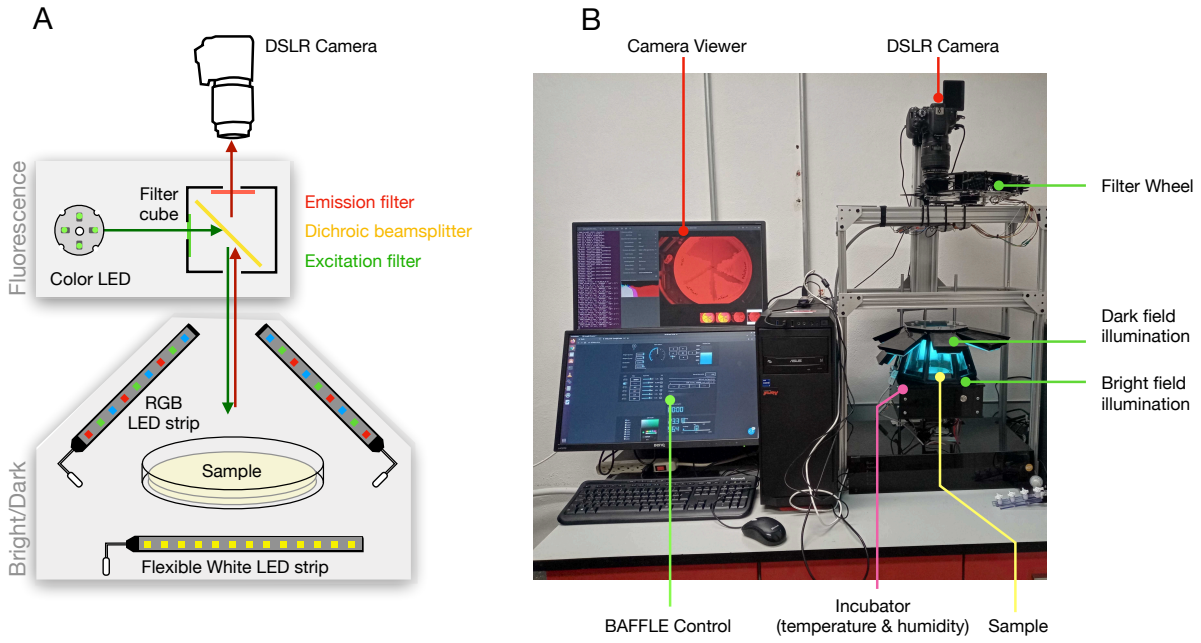

Figure 1: A) Schematic diagram of the device illustrating the fluorescent excitation and emission filters, as well as the bright and dark fields. B) Photograph of device (modules are color-coded: image acquisition and analysis in red, illumination in green, and incubator in pink).

Overall Implementation and design

The device described here was built using Open Hardware components and a standard DSLR camera. We use low-cost electronics to interface with all analog and digital inputs/outputs (e.g. sensors, switches and LEDs), as well as to control the Nema-17 stepper motors moving the filter wheel and the vertical axis. When possible, we used OpenBuilds aluminum extrusion V-slot profiles, with standard screws, nuts

and joints (a complete list of components can be found in the project's repository [31]). The device also contains acrylic elements (cut using a GlowForge laser CNC) and 3D-printed parts (printed in PLA using a Ultimaker 3). All files necessary to cut acrylic and print PLA parts are provided as supplementary files.

The system is composed of the following modules: incubation, illumination, fluorescence, and image acquisition. All these modules are managed via a browser GUI (coded in Python-Dash [39]), that allows control and configuration over the set of parameters within each module. In that sense, the overall system can function ''on the fly" in a simple sample inspection mode or, as in the primary mode, as a long-term image acquisition system with a selected set of personalized parameters. The latter can be inserted into the GUI by the use of a customizable template.

(2) Quality control

Safety

The only safety issues relevant to the overall system are the ones regarding the incubator module. The peltier module used for the air heating can reach up to a very high temperature. To maintain the temperature within the standard user-defined values the temperature detector is coupled to a relay system that switches off once the nominal temperature is reached within the incubator. Moreover, the peltier module is inserted into an aluminum heater dissipator and encased within the incubator module which remains isolated to prevent any kind of direct physical contact. As well the 12V-30A power supply that powers most of the system is secluded.

Calibration

To calibrate our fluorescent-based approach to identify bacterial genotypes in space, we used a library of *Escherichia coli* K12 bacteria carrying a multicopy plasmid encoding for different fluorescent proteins[4]:

- **Red**: DsRed (excitation 558 nm/emission 584 nm)
- **Red**: E2Crimson (558 nm/583 nm)
- **Green**: GFPmut3 (500 nm/513 nm)
- **Yellow**: mVenus (515 nm/527 nm)
- **Cyan**: sCFP-A3 (433 nm/474 nm)
- **Non-fluorescent control**.

We streaked each strain (see Table 2 for details) into a Petri dish filled with semi-solid LB agar and incubated overnight. Figure 2A illustrates the acquired images using Bright and Dark fields (white light, with back and front illumination, respectively). We also acquired images using different filters and LED configurations (hereafter referred to as *fluorescent channels*): red (excitation 559 nm/emission 630 nm), green (469 nm/525 nm), cyan (434 nm/479 nm) and yellow (497 nm/535 nm).

Normalized fluorescent intensities for each channel were obtained by subtracting the background and dividing the intensity of each pixel by the maximum fluorescence intensity of the whole image (ImageJ macros used for image analysis can be downloaded from the project's GitHub repository [31]). Figure 2B shows the multi-channel image and Figure 2C the resulting composite image. Note how each strain emits light at a specific wavelength that is detectable by a combination of channels. In the following section we will illustrate how this information can be used to estimate the temporal and spatial distribution of fluorescent strains.

(3) Application

Although microbial communities have a direct impact in human health [2] and ecosystem sustainability [1], as well as bio-engineering applications [24], understanding the ecological dynamics that emerges between

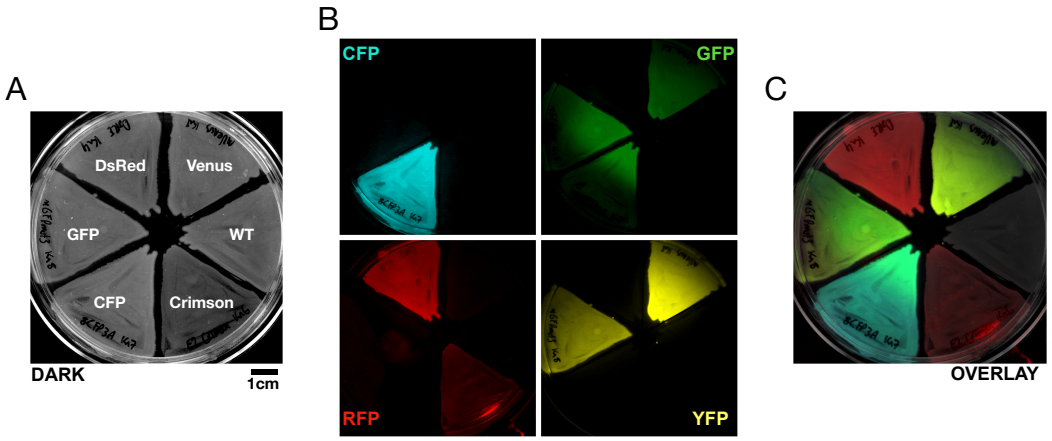

Figure 2: A) Dark-field image of a Petri dish inoculated with different fluorescent strains of *E. coli* (see Table 2 for a complete list of strains). B) Montage of images acquired using different fluorescent channels: CFP (cyan), GFP (green), YFP (yellow) and RFP (red). C) Overlay image produced by blending different fluorescent channels over the dark-field image.

different individuals within a complex microbial community remains a challenging problem[13]. Actually, it has even been suggested that the key limitation of applying ecological theory to study microorganisms is the difficulty of observing microbial communities in ecological settings [34].

A previous study showed that fluorescent microscopy can be used to evaluate the spatial arrangement of different fluorescent strains within the millimeter range [20]. Here we use a similar approach, but using a standard DSLR camera instead of a stereomicroscope, to obtain data on growth and morphology of expanding bacterial colonies from time-lapse images. From these multi-channel images we can then quantify fitness of different fluorescent subpopulations growing in spatially-explicit environments. To illustrate its capabilities, we will describe a series of examples where multi-channel images obtained with our device are used to characterize multiple aspects of the population dynamics resulting from the complex spatial arrangement exhibited during surface colonization.

Use case: Quantifying bacterial fitness from pair-wise competition assays

There are multiple methods to estimate *fitness* of bacterial populations [43]. For instance, many experimental studies quantify bacterial fitness by growing strains separately and comparing their maximum growth rate, a quantity that can be obtained from the optical density of a well-mixed culture [18]. A clear benefit of this approach is that it can be performed in high-throughput using microwell plate readers, thus obtaining periodic measurements of hundreds of samples while growing under controlled temperature and humidity conditions. However, this approach also has many limitations, as it ignores any growth promotion or inhibition compounds produced by other strains when grown in co-culture and, more importantly, only measures one component of fitness.

An alternative approach to quantify fitness is to grow multiple strains in co-culture and directly measure their relative abundances. This method is based on a pair-wise competition between different strains for limited resources and therefore can be used to determine whether one strain has a fitness advantage over another, thus providing a relative fitness measure instead of absolute fitness. There are, of course, limitations associated with this approach, mainly because we need to be able to identify different cells in a mixed culture. In some cases, specific members of the community can be identified through their morphology in agar plates or by their ability to grow in selective media, although this approach is not always reliable and only works in specific cases.

Another possibility is to use fluorescent markers to identify target subpopulations within multi-species microbial communities. Figure 3A shows an experiment that consists of a co-culture of two *E. coli* strains

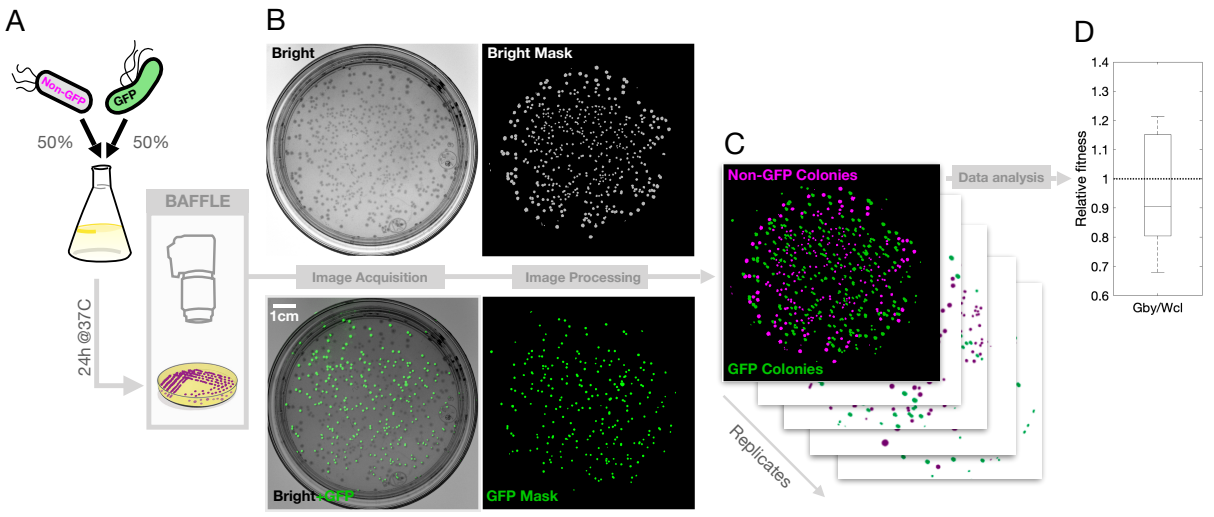

Figure 3: Diagram illustrating a pair-wise competition experiment. A) A 50-50 culture of fluorescent and non-fluorescent strains is inoculated into rich medium. After growing 24 hours under constant temperature and agitation, a sample is obtained, diluted and spread onto a Petri dish with semi-solid media. B) Images obtained using Bright and GFP channels can be used to obtain binary masks. C) By evaluating the fluorescence of each colony identified in the masks, we estimate the number of colony forming units (CFUs) of each strain. D) Replicating this protocol multiple times allows us to estimate the relative fitness between the fluorescent and non-fluorescent strains.

[3], one of the strains was transformed with a well-characterized plasmid containing a gene encoding for a green fluorescent protein (GFP) [36]. After 24 hours of growth in rich media, the co-culture was diluted and plated in semi-solid agar with rich media. We incubated the Petri dishes at $37°C$ and estimated the abundance of each phenotype by counting the colony-forming units (CFUs) of each strain.

Figure 3B illustrates how image processing can be used to analyze multi-channel images (GFP and Bright channels). In particular, here we use image segmentation to obtain binary masks whereby black pixels belong to the background and white pixels correspond to a bacterial colony. By comparing Bright and GFP images, we then determine which colonies correspond to each strain, as illustrated in Figure 3C. Finally, a colony counting algorithm can be used to estimate the proportion of fluorescent colonies with respect to the total number of colonies. This information is very useful, as it enables us to estimate the Malthusian growth ratio between both strains (see Figure 3D), a fundamental quantity in experimental microbiology referred to as *relative fitness* [43].

Use case: Evaluating bacterial fitness in a gradient environment

A limitation of the competition assay discussed previously is that it is performed under a single environmental condition. In many circumstances, it is important to simultaneously evaluate the fitness of a bacterial population under a range of environmental conditions. For instance, to determine the critical concentration that suppresses the growth of clinically-relevant pathogens, a quantity known as the Minimum Inhibitory Concentration. This can be estimated with parallel competition assays in liquid media or using disk-diffusion assays in agar plates [21]. In the latter approach, bacterial susceptibility is determined by quantifying the zone of inhibition around an antibiotic source. Another benefit of this approach is that it allows to characterize the resistance profile of a bacterial isolate to multiple antimicrobial substances in a single Petri dish.

A series of laboratory studies have also used spatially-explicit environments to evaluate microbial evolutionary dynamics [5, 8] and to study gene expression in response to environmental gradients [17, 41]. To identify different genotypes from mixed cultures, a common approach is to isolate bacterial clones and

perform an analysis of DNA sequences of specific target genes that allow differentiating between different bacterial genotypes[22]. If using fluorescently-tagged strains, then the relative and absolute abundances of different strains can be estimated using spectrophotometry and flow cytometry [33, 25]. Note, however, that both of these approaches are invasive techniques that do not allow for dynamic measurements and long-term observations.

As our device allows us to evaluate the spatial distribution of bacteria with different fluorescent markers, then we can study the consequences of heterogeneous environments on the community dynamics. For example, antibiotic gradients produce a range of selective pressures for (and against) resistant (and susceptible) bacterial genotypes in different spatial locations, so we can use a drug gradient to evaluate the relative fitness between two strains. In a previous study, we designed a bespoke experimental system consisting of a spatially-explicit culture device built using 3D printing [16] whereby cells are immobilized in specific locations, but with antibiotics diffusing between neighboring compartments. Figure 4A illustrates another gradient device built from acrylic, whereby both cells and chemical substances can diffuse through space (SVG files used by the laser engraver can be obtained from the GitHub repository [31]).

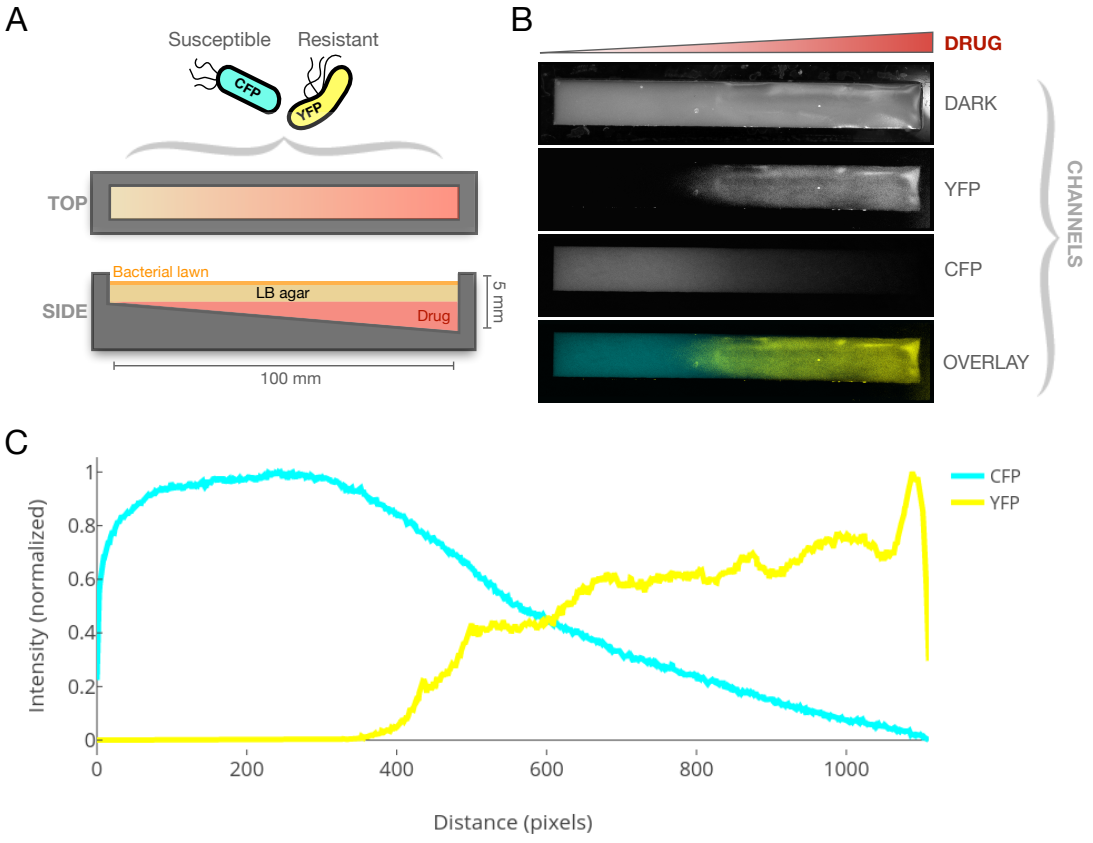

Figure 4: A) Diagram illustrating an antibiotic gradient experiment consisting in a co-culture of susceptible and resistant bacteria. A 50-50 culture of Cyan (susceptible) and Yellow (resistant) fluorescently-tagged bacteria are inoculated homogeneously in the surface of the agar. B) Multi-channel image acquisition is performed after 48h of incubation, from top to bottom: Dark, YFP, CFP and an overlay image of both fluorescent channels. C) Relative population abundance can be quantified in space based on the normalized fluorescent intensity detected in each channel.

We filled the bottom part of the gradient device with semi-solid agar supplemented with a lethal dose of antibiotic ($50\mu g/ml$ of *kanamycin*, an aminoglycoside bactericidal drug), and once it has solidified, we then pour drug-free LB agar medium on top. After storing for a couple of days at $4°C$, an antibiotic gradient is formed, and we inoculate with a co-culture of *E. coli* bacteria uniformly over the agar surface. We denote our strains Gby and Wcl, which are susceptible and resistant to the antibiotic, respectively. Both strains encode different fluorescent markers (YFP in Gby, CFP in Wcl) [10, 11], so we estimated the spatial distribution of each strain by analyzing multi-channel fluorescent images obtained after 48 hours

of incubation at $37°C$ (see Figure 4B). As expected, a consequence of a drug gradient is the formation of a landscape of selective pressures that modulates the spatial distribution of each strain. Indeed, Figure 4C shows that, at high drug concentrations, the population consists exclusively of drug-resistant cells (yellow), while at low antibiotic concentrations the resistant subpopulation is outcompeted by the susceptible strain, and thus the population consists of drug-sensitive cells (cyan).

Use case: Evaluating colony expansion within a 3-strain bacterial consortium

To illustrate that multi-channel images acquired with this device can be used to estimate the spatial distribution of different bacterial strains within a multi-species community, we use a previously characterized resistance-motility microbial consortia[14]. *Paenibacillus sp.* is a soil bacterium with a social organization based on physical and chemical signaling [7, 35]. Some *Paenibacillus sp.* (e.g. *P. vortex* and *P. lautus*) are known to generate complex spatial patterns consisting of vortices of thousands of cells that serve as building blocks for new colonies [23, 40]. To maintain cohesion of the vortices, flagella of *Paenibacillus sp.* tend to intertwine with the flagella of neighboring cells [15]. As a result, other organisms are dragged with the rapidly expanding colony. For instance, it has been reported that *P. vortex* is capable of transporting photosynthetic algae when food resources are scarce in order to consume them later, as well as transporting recombinant *E. coli* with useful properties, such as the expression of β-galactosidases and cellulases that enhance resource uptake from the environment [7, 32].

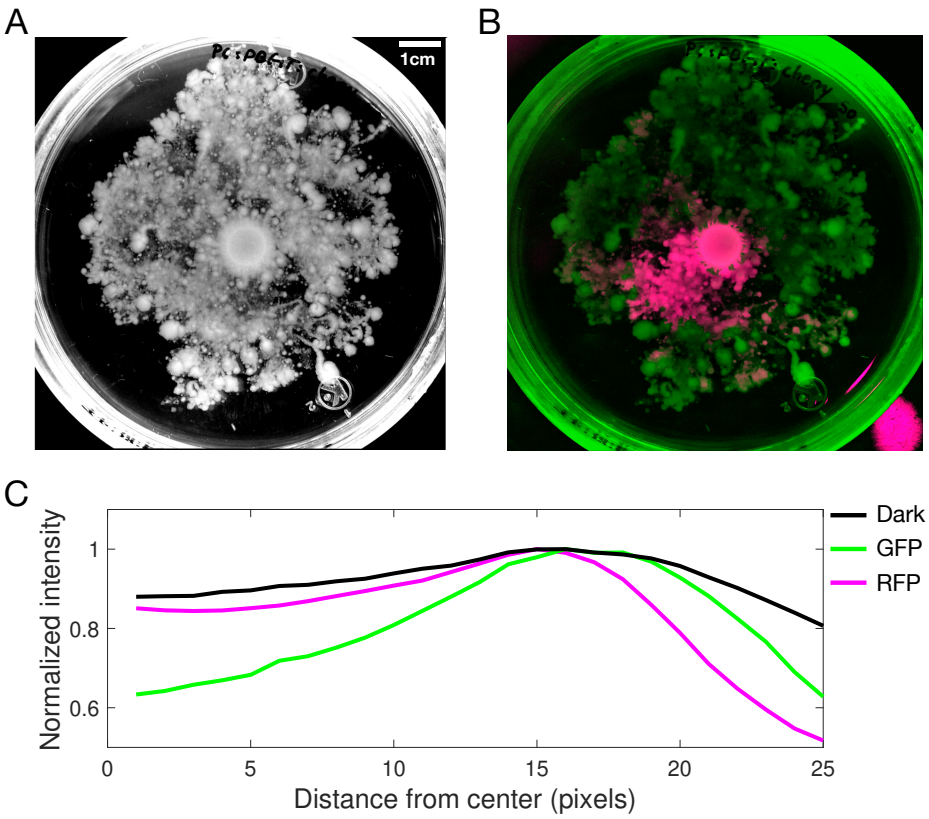

Figure 5: Multi-channel image illustrating a 3-strain bacterial co-culture in an agar plate containing LB medium ($1.5g/l$) and a lethal dose of antibiotic (50μg/ml of ampicillin). A) Dark field image showing a swirling-tree morphology. B) Fluorescent channel overlay image showing the spatial distribution of both *E. coli* strains: resistant in green and susceptible in magenta. C) Plot showing the normalized intensity in concentric rings around the center: dark field in black (*P. lautus*), GFP in green (resistant *E. coli*), and RFP in magenta (susceptible).

In particular, we use a bacterial consortium composed of a non-motile drug-susceptible *E. coli* (magenta), a non-motile drug-resistant *E. coli* (green), and a motile drug-susceptible *P. lautus* (non-fluorescent). In the presence a β-lactam antibiotic [30], a mutualistic interaction emerges between the resistant *E. coli* and *P. lautus*; the previous produces a β-lactamase that locally degrades the antibiotic, thus allowing the latter to expand its growing domains. Figure 5A shows that the spatial pattern produced by this

resistance-motility consortium are concentric rings resulting from periods of reduced and accelerated expansion, coinciding respectively with the detoxification of the medium by *E. coli* and the subsequent swarming of *P. lautus*. Figure 5B shows that, during colony expansion, both types of *E. coli* cells (green and red) are dragged short distances, but only the resistant strain can be found in the colony edges, as shown in Figure 5C.

Use case: Quantifying spatio-temporal changes in colony morphology

Within the dark field configuration, the system can also be used as a macro and extreme macro photography studio platform with other biological specimens than bacterial colonies, as it allows the performance of image stacking techniques via a micrometric control of the stage position with respect to the camera by the use of an stepper motor and a customized lightning setup.

Figure 6A shows a time-lapse obtained from an experiment consisting on the growth of a bacterial colony of *Paenibacillus dendritiformis* (type T) in an agar plate. This swarming strain is known to develop a diversity of patterns mostly affected by the nutrient level and hardness of the medium [6]. In our experiment, we used a peptone nutrient medium that contained NaCl (5 g/liter), K2HPO4 (5 g/liter), Bacto peptone (1 g/liter), and finally Difco agar was added at a concentration of 1.5% (wt/vol).

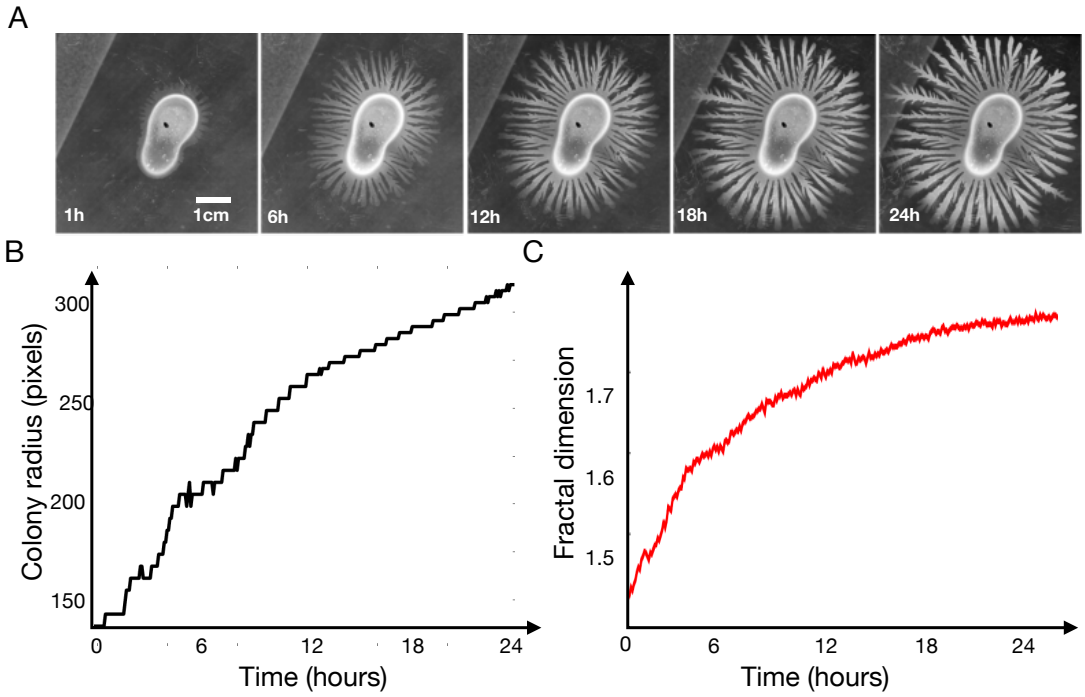

Figure 6: Figure illustrating the growth of the pattern-forming bacteria *Paenibacillus dendritiformis*. A) Selected time-lapse frames along its growth showing that the extrusion of the main branches over the inoculum initial contour remains fixed over time, while its tips expand radially and form more branches in a self-similar way. B) Colony expansion quantified as the maximum distance achieved by the colony in time. C) Plot of the evolution of the computed fractal dimension during growth, smoothly converging towards an expected D=1.767 value.

Time-lapse images can also be used to analyze expansion of a growing colony. Figure 6B shows how the colony radius (here defined as the maximum distance reached by a dendrite to the center of the colony) increases in time. Moreover, within this low nutrient and hard medium regime, the bacterial colony is know to produce a self-similar branching morphology through a diffusion-limited process, which can be quantified using fractal dimension methods. By using a box counting algorithm, we obtained a fractal dimension of the colony patterns of $D = 1.767$, very close to that of the two-dimensional DLA model and previous experimental reports around $D = 1.73$ [27] (see Figure 6C).

Reuse potential and adaptability

In our device, we used four specific excitation/emission filters and LEDs. To detect different fluorescent proteins, the appropriate filters and LEDs would need to be acquired.

(4) Build Details

Fluorescence excitation

The fluorescent excitation module is build around a commercial design composed of filter cubes, for instance Microscopy Filter Cubes with Pre-Installed Fluorescence Filters by Thorlabs. A collection of Creative Commons fluorescent filter cubes for microscopy can be found in Thingiverse. As illustrated in Figure 7A, each one of the four cubes holds a fluorescence filter set, including an excitation filter (Figure 7C in blue), emission filter (Figure 7C in purple), dichroic mirror (Figure 7B top) and finally an illumination source.

The fluorescent illumination consists in high-intensity Rebel 23mm Quad LEDs with specific wave-lengths: Red (627nm), Amber (590nm), Cyan (505nm) and Blue (470nm). The four fluorescent channels as seen in Figure 7C include excitation filters (mounted in the blue lateral part), and emission filters (mounted in the purple top side): Red (excitation 559 nm/emission 630 nm), Green (469 nm/525 nm), Cyan (434 nm/479 nm) and Yellow (497 nm/535 nm).

As seen in Figure 7B the filter wheel holds all four fluorescence cubes equally spaced together with a hole (seen in the top red and bottom green acrylic layers) that is used for the dark/bright field illumination. A Nema17 stepper motor slowly rotates the filter around its central axis, clockwise or counterclockwise according the time-lapse setup.

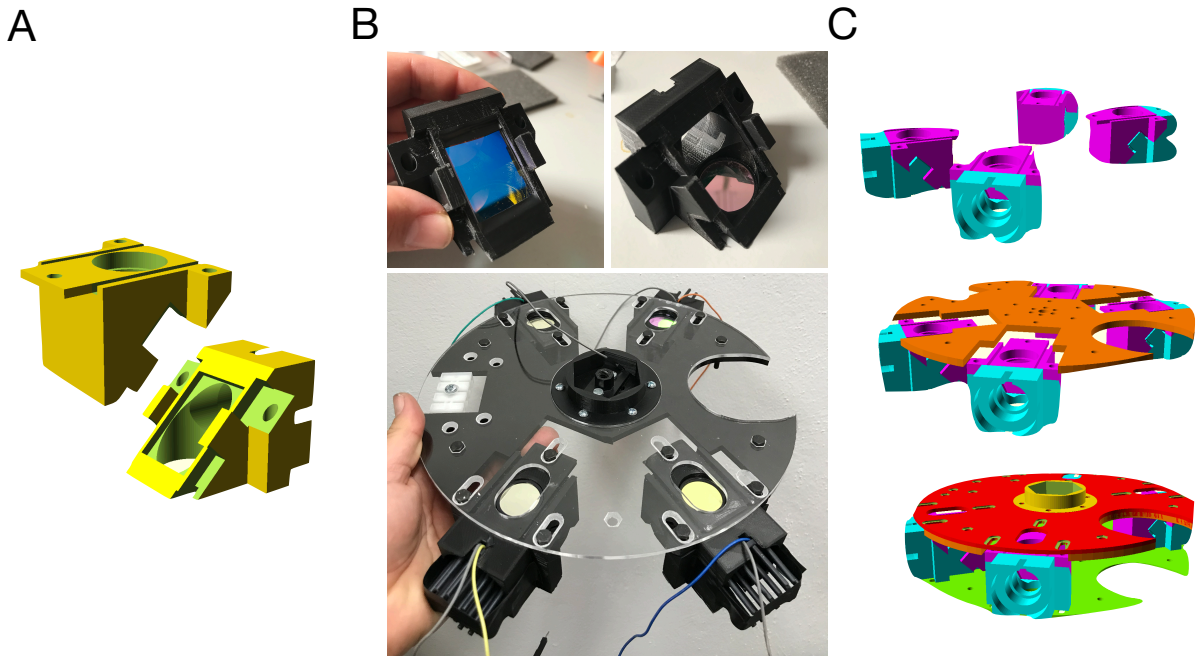

Figure 7: Fluorescence wheel module. A) CAD file of the filters cubes which hold on top the emission filter and on the lateral the excitation filter. B) Photography of the dichroic mirror placement in between the two parts of the fluorescent cubes. C) CAD design of the filter wheel system containing the four fluorescent cubes.

Image acquisition and analysis

To acquire high-resolution images, we used a standard DSLR camera (Canon T6i) with a macro lens (100mm). Support for the camera is based on a 3D-printed FlexTILT head by Edelkrone (https://edelkrone.com/products/flextilt-head-v3). Camera is controlled from a computer through the open-source software Entangle (https://entangle-photo.org/). We also have a remote control to shoot from our software. Focus is achieved by moving the stage vertically through a linear actuator with a lead screw (for instance, this V-Slot NEMA 17 Linear Actuator Bundle).

Flat field correction may be used when illumination is not even, specially in the case of fluorescent imaging mode, since there may be some dealignment between the fluorescent filter cube and the optical lens of the DSLR camera. Standard flat field corrections can be performed with any post processing image software, such as ImageJ, by taking a background image without the sample and then measuring the mean intensity in order to perform a normalization between images. Moreover, some ImageJ plugins such as https://imagej.net/plugins/bigstitcher/flatfield-correction offer on-the-fly correction for a user-provided dark image and/or bright image.

Semi-automated image analysis can be performed using any image processing software. In particular, we used ImageJ [37] to produce Figures 3-6, with scripts that can be downloaded from the project's GitHub repository [31].

Incubation

In order to maintain temperature in ideal conditions for bacterial growth (usually $30\,\mathrm{deg}\,C$ or $37\,\mathrm{deg}\,C$), we use an Arduino-based (Arduino Mega2560 + Shield) thermostat build around a system that contains a temperature and humidity sensor (Grove - Temperature and Humidity Sensor (High-Accuracy and Mini) v1.0) and a relay that controls a heat source attached to a series of heat dissipators. Hot air is then introduced into the incubation chamber through 8cm fans. The incubation box is made of 5mm acrylic attached to a V-slot frame through 3D-printed joints. Temperature data from the sensor is continuously read by the GUI, which compares it regularly with the user-selected temperature to active or deactivate the relay connected to the heat source. Similarly, we implemented a humidity control system that actuates an ultrasonic mist maker once the humidity goes below the humidity parameter value selected by the user.

Illumination

For the dark field illumination setup, we use an 8-segment addressable LED strip with 48 light points in total (6 LED's x 8 segments) directed towards the sample with different incident light angles in a diffused manner via a semi-transparent acrylic sheet. These standard 12 Volt WS2812 low-cost LED fixtures are programmed through FastLED Arduino library (https://fastled.io/). This allows us to define RGB and alpha characteristics of the light in a customizable way for each of the 8 segments according to the user's preferences using serial communication through Python scripting between the GUI and the Arduino controller. For the bright field setup, we use standard white LED non-addressable fixtures which are situated under the semi-transparent acrylic plate that holds the sample. It may be helpful in some situations to incorporate the use of RGB addressable LEDs also within the bright field configuration. The possibility of changing the transmitted light color and its intensity may be useful for instance to have some further flexibility in the balance of the camera aperture and exposure configuration. For that reason it may be easily implemented as an upgrade in future versions of the device, using the same Arduino based configuration as in the dark field mode.

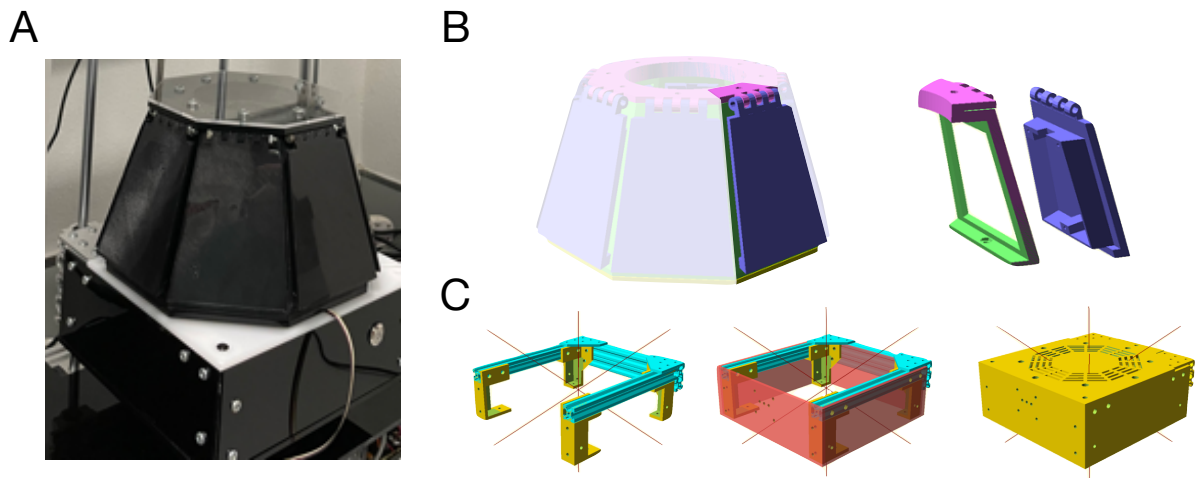

Figure 8: A) Photo of incubation/illumination chamber. B) The illumination chamber is composed of eight segments with addressable LEDs that can be controlled independently. C) Structure of the incubation chamber where the heat source and fan are contained. This box also contains the white LEDs used for back illumination (bright field).

Operating software

We developed a Python-based GUI using DASH components (https://dash.plotly.com/dash-core-components), allowing us to control the device through a standard web browser. This software allows to separately control color and intensity of each segment in the dark light module, as well as of the fluorescent LEDs and the position of the filter wheel.

To trigger the camera shutter we use a standard remote control shutter release cable. So, by setting the camera to Bulb, we then control each individual optical configuration speed by setting the exposure time into the slider position.

This system allow us to work with multiple independent optical configurations within the same time-lapse experiment. For instance, one can define a setup composed of 5 instances:

- Bright Field (1 sec exposure)
- Dark Field (white #f0f8ff color, 0.01 sec exposure)
- Dark Field (yellow #fdff00 color, 0.5 sec exposure)
- Cyan Fluorescence (5 sec exposure)
- Red Fluorescence (20 sec exposure)

This instances are going to be performed sequentially each time interval defined within the time-lapse box timer and with the temperature and humidity set at the subsequent sliders. In order to interface the digital camera to the computer we use the mentioned open-source software Entangle, which provides live image preview and a graphical interface for tethered shooting.

Moreover, some of the most relevant internal processes performed during the duration of the experiment, such as temperature and humidity readouts and motor movements, are printed into the terminal log in order to maintain a time-stamp register of all the actions. Finally, the device runs an Ubuntu 20.04.3 LTS Linux 64 bits OS with an Intel Core i7-11700 @ 2.50GHz x 16 processor, 62GiB of memory and 2TB of disk capacity.

Dependencies

In order to 3D print the designs a slicing software such as Ultimaker Cura2 is required to convert the provided .stl files into g-code. All .stl files for 3D printing were created through parametric modeling and can be modified using OpenScad [26].

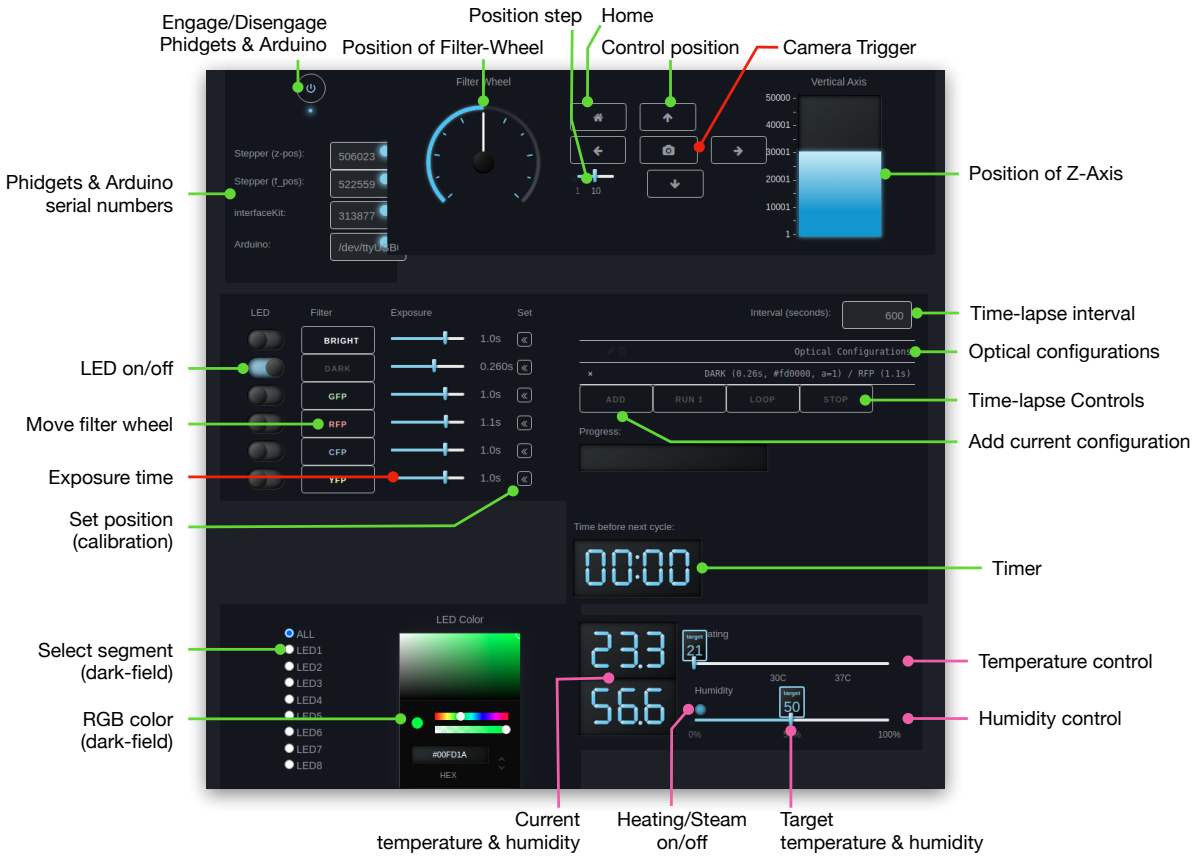

Figure 9: Screenshot of the graphical browser user interface that provides an interactive method to control the device settings and preferences. The green arrows point to the illumination controls, red arrows to the camera and in pink arrows to the incubator module.

The GUI was written in Python and depends on various common libraries (pandas, numpy, time). We use a Plotly-based framework to display the web app (Dash and Dash Core Components; https://github.com/plotly/dash). Phidget22 is used to control the stepper motors (https://pypi.org/project/Phidget22/). FastLED is used to control the addressable LED strip (https://github.com/FastLED/FastLED).

Hardware documentation and files location

Name: GitHub
Persistent identifier: https://github.com/ccg-esb-lab/BAFFLE/
Licence: MIT License
Publisher: Rafael Peña-Miller
Date published: 28/02/2022

(5) Discussion

The use of dark/bright field and fluorescent macroscopic imaging techniques in controlled environments and within the millimeter range constitutes an essential tool in order to develop studies focused on bacterial colony growth and biofilm formation in spatially explicit environments. Yet, hardware and software instrumentation within microbiology research domains is often expensive and restricted, leading to a

narrow use outside wealthy research institutions and academic labs. On the other hand, the increasing availability of open source microcontrollers and customizable manufacturing technologies has facilitated the development of inexpensive scientific devices and laboratory equipment both inside and outside traditional microbiology lab environments, such as in high schools, DIY-DIWO movements (Do It Yourself, Do It With Others), amateur microscopy groups, maker spaces and biofablabs, and within ecology and bioart collectives.

By following this open hardware and open source software ethos, we have developed an image acquisition device with the aim of acquiring time-lapse macro images of Petri dishes by the use of an inexpensive, reliable and tunable system. In that sense our system can be used to function both in a single-channel or multi-channel configuration, and both in a dark field or multi-fluorescence light arrangement. Moreover, in order to allow for controlled growth conditions that permit to obtain reproducible observations in long term duration experiments, the system allows to set-up different environmental configurations that can also be variable in time.

In order to test our imaging system overall functionalities, we have investigated its scope and limitations on several experimental cases that had the need of spatio-temporal tracking and quantification of both non-fluorescence and multiple fluorescence signals. Besides those explored trials we think that the modularity of our systems may allow to perform other type of non bacterial growth experiments such as the tracking of plasmodium filaments in amoebozoa organisms, the formation of mycelium fungal networks or even root system architectures in plants.

A last thought, regarding the overall building experience of such a device, goes into acknowledging its entangled multi-disciplinary technical aspects and human expertise sides. By gathering a collaborative group effort made of individual know-how insights, ranging from DIY building designs to synthetic biology plasmid transformation techniques, what finally emerges is represented, as greater than the sum of the parts, not as the device itself but rather as an horizontal transfer of knowledge's along a shared path. Being so, this kind of projects can be framed not only as empowering observational tools to be used by underrepresented (academic and non-academic) collectives but also as experimental educational practices shaped within the community.

Future Work

One of the difficulties encountered while using the humidity control of the incubator via the mist maker is the formation of water condensation droplets upon the transparent acrylic cover resulting in blurred images. In order to prevent this issue, we are currently working in the use of an anti-fog coating sheet layer that removes the fog once a small current is applied to it.

The aperture control system of the DSLR camera that we use it is not allowed to vary along each time-lapse optical configuration. This turns out to be not optimal when working for instance with combined dark/bright field and fluorescent modes, since the former requires a small aperture in order to improve the depth of field of the image and the latter requires a big aperture in order the capture the fluorescent light which is fainter.

Last but not least, we find important to mention that even we tagged the device as being "low-cost" by comparing it to similar commercial versions, the use of a DSLR camera and it's optics together with an state-of-the-art computer makes the overall system out of the budget for a wide proportion of users. For all that, all the software can in fact run into tiny and affordable computers, such as Raspberry Pi models, and its corresponding Raspberry Pi High Quality Cameras, which ultimately turns out to drop the general price of the device.

Paper author contributions

CTP and RPM designed and assembled this device. CTP, DRG, FS, AFD and RPM performed experiments and analysed the data. RPM and AFH assembled and tested earlier versions of this device. All

authors contributed to discussions and writing of the manuscript.

Acknowledgements

We thank Michael Sieber, Fernán Federici, Remi Chait and Rob Beardmore for inspiration and useful discussions. We also thank Christian Sohlenkamp, David Zamorano, Juan Keymer and Lourdes Girard for providing bacterial strains and advice. We also appreciate the help and input from past and present members of the Systems and Synthetic Laboratory at CCG-UNAM.

Funding statement

This work was supported by CONACYT (Ciencia Básica grant A1-S-32164) and by PAPIIT-UNAM (grants IN209419). DRG is a doctoral student in Programa de Doctorado en Ciencias Biomédicas, Universidad Nacional Autónoma de México, and received fellowship 572373 from CONACYT.

Competing interests

The authors declare that they have no competing interests.

References

[1] E Abatenh, Birhanu Gizaw, Z Tsegaye, and Genene Tefera. Microbial function on climate change–a review. *Open Journal of Environmental Biology*, 3(1):001–007, 2018.

[2] Virginia Robles Alonso and Francisco Guarner. Linking the gut microbiota to human health. *British Journal of Nutrition*, 109(S2):S21–S26, 2013.

[3] Tomoya Baba, Takeshi Ara, Miki Hasegawa, Yuki Takai, Yoshiko Okumura, Miki Baba, Kirill A Datsenko, Masaru Tomita, Barry L Wanner, and Hirotada Mori. Construction of escherichia coli k-12 in-frame, single-gene knockout mutants: the keio collection. *Molecular systems biology*, 2(1), 2006.

[4] Enrique Balleza, J Mark Kim, and Philippe Cluzel. Systematic characterization of maturation time of fluorescent proteins in living cells. *Nature methods*, 15(1):47–51, 2018.

[5] Michael Baym, Tami D Lieberman, Eric D Kelsic, Remy Chait, Rotem Gross, Idan Yelin, and Roy Kishony. Spatiotemporal microbial evolution on antibiotic landscapes. *Science*, 353(6304):1147–1151, 2016.

[6] Avraham Be'er, Rachel S Smith, HP Zhang, E-L Florin, Shelley M Payne, and Harry L Swinney. Paenibacillus dendritiformis bacterial colony growth depends on surfactant but not on bacterial motion. *Journal of bacteriology*, 191(18):5758–5764, 2009.

[7] Eshel Ben-Jacob. My encounters with bacteria—learning about communication, cooperation and choice. *Physical biology*, 11(5):053009, 2014.

[8] Jesús Blázquez, Alejandro Couce, Jerónimo Rodríguez-Beltrán, and Alexandro Rodríguez-Rojas. Antimicrobials as promoters of genetic variation. *Current opinion in microbiology*, 15(5):561–569, 2012.

[9] André Maia Chagas. Haves and have nots must find a better way: The case for open scientific hardware. *PLoS biology*, 16(9):e3000014, 2018.

[10] Remy Chait, Allison Craney, and Roy Kishony. Antibiotic interactions that select against resistance. *Nature*, 446(7136):668–671, 2007.

[11] Remy Chait, Shreya Shrestha, Aakash Kaushik Shah, Jean-Baptiste Michel, and Roy Kishony. A differential drug screen for compounds that select against antibiotic resistance. *PloS one*, 5(12):e15179, 2010.

[12] Maria Peñil Cobo, Silvia Libro, Nils Marechal, David D'Entremont, David Peñil Cobo, and Mehmet Berkmen. Visualizing bacterial colony morphologies using time-lapse imaging chamber mocha. *Journal of bacteriology*, 200(2), 2018.

[13] Sylvie Estrela, Jean C.C. Vila, Nanxi Lu, Djordje Bajić, Maria Rebolleda-Gómez, Chang-Yu Chang, Joshua E. Goldford, Alicia Sanchez-Gorostiaga, and Álvaro Sánchez. Functional attractors in microbial community assembly. *Cell Systems*, 13(1):29–42.e7, 2022.

[14] Alin Finkelshtein, Dalit Roth, Eshel Ben Jacob, and Colin J Ingham. Bacterial swarms recruit cargo bacteria to pave the way in toxic environments. *MBio*, 6(3):e00074–15, 2015.

[15] Alin Finkelshtein, Alexandra Sirota-Madi, Dalit Roth, Colin J Ingham, and Eshel Ben Jacob. Paenibacillus vortex—a bacterial guide to the wisdom of the crowd. In *Biocommunication: sign-mediated interactions between cells and organisms*, pages 257–283. World Scientific, 2017.

[16] Ayari Fuentes-Hernández, Anastasia Hernández-Koutoucheva, Alán F Muñoz, Raúl Domínguez Palestino, and Rafael Peña-Miller. Diffusion-driven enhancement of the antibiotic resistance selection window. *Journal of the Royal Society Interface*, 16(158):20190363, 2019.

[17] Ee-Been Goh, Grace Yim, Wayne Tsui, JoAnn McClure, Michael G Surette, and Julian Davies. Transcriptional modulation of bacterial gene expression by subinhibitory concentrations of antibiotics. *Proceedings of the National Academy of Sciences*, 99(26):17025–17030, 2002.

[18] Barry G Hall, Hande Acar, Anna Nandipati, and Miriam Barlow. Growth rates made easy. *Molecular biology and evolution*, 31(1):232–238, 2014.

[19] Raimo Hartmann, Hannah Jeckel, Eric Jelli, Praveen K Singh, Sanika Vaidya, Miriam Bayer, Daniel KH Rode, Lucia Vidakovic, Francisco Díaz-Pascual, Jiunn CN Fong, et al. Quantitative image analysis of microbial communities with biofilmq. *Nature microbiology*, 6(2):151–156, 2021.

[20] Theresa Hölscher, Anna Dragoš, Ramses Gallegos-Monterrosa, Marivic Martin, Eisha Mhatre, Anne Richter, and Ákos T Kovács. Monitoring spatial segregation in surface colonizing microbial populations. *JoVE (Journal of Visualized Experiments)*, (116):e54752, 2016.

[21] RA Howe and JM Andrews. Bsac standardized disc susceptibility testing method (version 11). *Journal of antimicrobial chemotherapy*, 67(12):2783–2784, 2012.

[22] Luisa W Hugerth and Anders F Andersson. Analysing microbial community composition through amplicon sequencing: from sampling to hypothesis testing. *Frontiers in microbiology*, 8:1561, 2017.

[23] Colin J Ingham and Eshel Ben Jacob. Swarming and complex pattern formation in paenibacillus vortex studied by imaging and tracking cells. *BMC microbiology*, 8(1):1–16, 2008.

[24] Nathan I Johns, Tomasz Blazejewski, Antonio LC Gomes, and Harris H Wang. Principles for designing synthetic microbial communities. *Current Opinion in Microbiology*, 31:146–153, 2016.

[25] Christin Koch, Susanne Günther, Adey F Desta, Thomas Hübschmann, and Susann Müller. Cytometric fingerprinting for analyzing microbial intracommunity structure variation and identifying subcommunity function. *Nature protocols*, 8(1):190–202, 2013.

[26] Felipe Machado, Norberto Malpica, and Susana Borromeo. Parametric cad modeling for open source scientific hardware: Comparing openscad and freecad python scripts. *Plos one*, 14(12):e0225795, 2019.

[27] Mitsugu Matsushita and Hiroshi Fujikawa. Diffusion-limited growth in bacterial colony formation. *Physica A: Statistical Mechanics and its Applications*, 168(1):498–506, 1990.

[28] Andrew R Miller, Gregory L Davis, Z Maria Oden, Mohamad Reza Razavi, Abolfazl Fateh, Morteza Ghazanfari, Farid Abdolrahimi, Shahin Poorazar, Fatemeh Sakhaie, Randall J Olsen, et al. Portable, battery-operated, low-cost, bright field and fluorescence microscope. *PloS one*, 5(8):e11890, 2010.

[29] Isaac Nuñez, Tamara Matute, Roberto Herrera, Juan Keymer, Timothy Marzullo, Timothy Rudge, and Fernán Federici. Low cost and open source multi-fluorescence imaging system for teaching and research in biology and bioengineering. *PloS one*, 12(11):e0187163, 2017.

[30] Michael I Page. The mechanisms of reactions of. beta.-lactam antibiotics. *Accounts of Chemical Research*, 17(4):144–151, 1984.

[31] R Peña Miller. ccg-esb-lab/baffle: v3.2-review (v3.2). https://doi.org/10.5281/zenodo.6960207, 2022.

[32] Mark Polikovsky, Eshel Ben-Jacob, and Alin Finkelshtein. P. vortex-mediated strategies for polysaccharides decomposition. *Technology*, 3(02n03):80–83, 2015.

[33] Ruben Props, Pieter Monsieurs, Mohamed Mysara, Lieven Clement, and Nico Boon. Measuring the biodiversity of microbial communities by flow cytometry. *Methods in Ecology and Evolution*, 7(11):1376–1385, 2016.

[34] James I Prosser, Brendan JM Bohannan, Tom P Curtis, Richard J Ellis, Mary K Firestone, Rob P Freckleton, Jessica L Green, Laura E Green, Ken Killham, Jack J Lennon, et al. The role of ecological theory in microbial ecology. *Nature Reviews Microbiology*, 5(5):384–392, 2007.

[35] Dalit Roth, Alin Finkelshtein, Colin Ingham, Yael Helman, Alexandra Sirota-Madi, Leonid Brodsky, and Eshel Ben-Jacob. Identification and characterization of a highly motile and antibiotic refractory subpopulation involved in the expansion of swarming colonies of p aenibacillus vortex. *Environmental microbiology*, 15(9):2532–2544, 2013.

[36] Alvaro San Millan, Jose Antonio Escudero, Danna R Gifford, Didier Mazel, and R Craig MacLean. Multicopy plasmids potentiate the evolution of antibiotic resistance in bacteria. *Nature ecology & evolution*, 1(1):1–8, 2016.

[37] Johannes Schindelin, Ignacio Arganda-Carreras, Erwin Frise, Verena Kaynig, Mark Longair, Tobias Pietzsch, Stephan Preibisch, Curtis Rueden, Stephan Saalfeld, Benjamin Schmid, et al. Fiji: an open-source platform for biological-image analysis. *Nature methods*, 9(7):676–682, 2012.

[38] James P Sharkey, Darryl CW Foo, Alexandre Kabla, Jeremy J Baumberg, and Richard W Bowman. A one-piece 3d printed flexure translation stage for open-source microscopy. *Review of Scientific Instruments*, 87(2):025104, 2016.

[39] Carson Sievert. *Interactive web-based data visualization with R, plotly, and shiny*. CRC Press, 2020.

[40] Alexandra Sirota-Madi, Tsviya Olender, Yael Helman, Colin Ingham, Ina Brainis, Dalit Roth, Efrat Hagi, Leonid Brodsky, Dena Leshkowitz, Vladimir Galatenko, et al. Genome sequence of the pattern forming paenibacillus vortex bacterium reveals potential for thriving in complex environments. *BMC genomics*, 11(1):1–16, 2010.

[41] Thuy Do Thi, Elena López, Alexandro Rodríguez-Rojas, Jerónimo Rodríguez-Beltrán, Alejandro Couce, Javier R Guelfo, Alfredo Castañeda-García, and Jesús Blázquez. Effect of reca inactivation on mutagenesis of escherichia coli exposed to sublethal concentrations of antimicrobials. *Journal of Antimicrobial Chemotherapy*, 66(3):531–538, 2011.

[42] Bas Wijnen, Emily E Petersen, Emily J Hunt, and Joshua M Pearce. Free and open-source automated 3-d microscope. *Journal of microscopy*, 264(2):238–246, 2016.

[43] Michael J Wiser and Richard E Lenski. A comparison of methods to measure fitness in escherichia coli. *PloS one*, 10(5):e0126210, 2015.

Copyright notice

Supplementary Figures

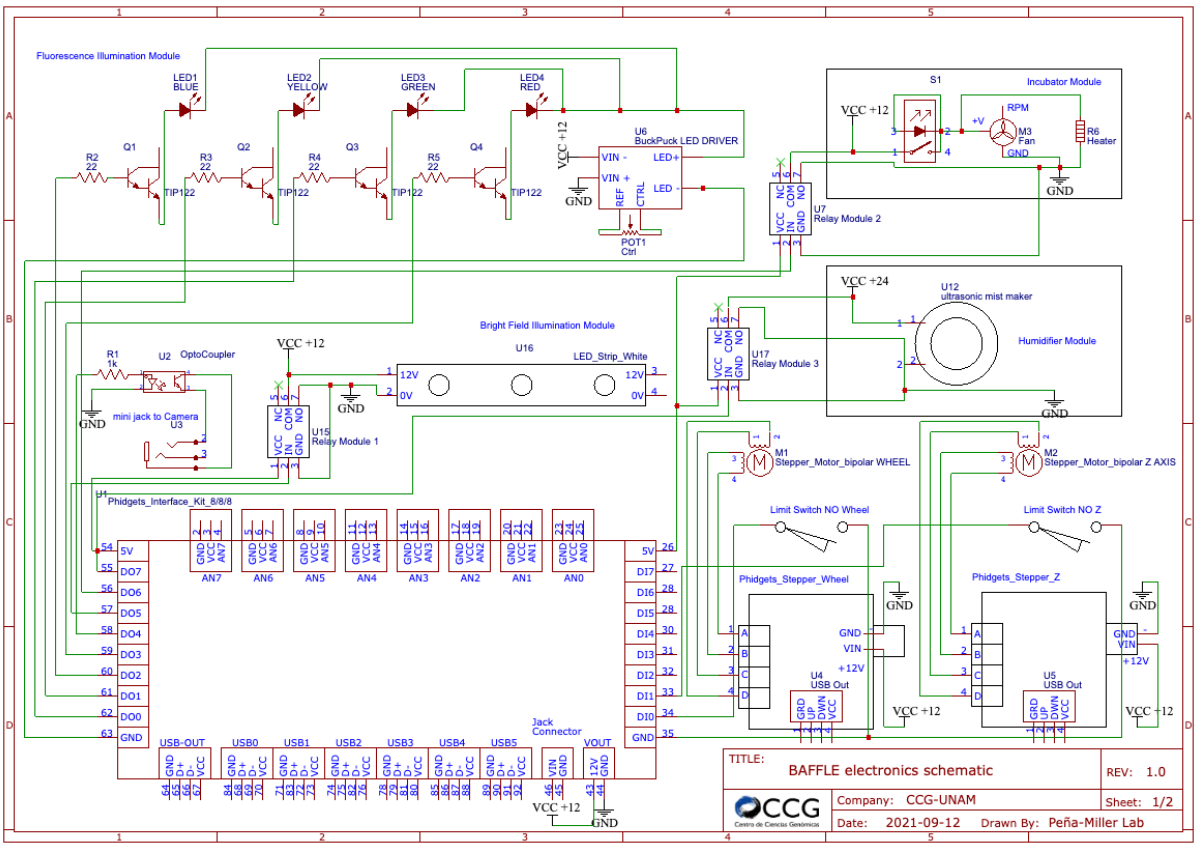

Figure 10: Electronic schematic diagram of the fluorescence and bright field illumination modules. Stepper control is achieved with a Phidgets Stepper Bipolar HC. Analog and digital inputs/outputs are controlled through a Phidgets Interface Kit.

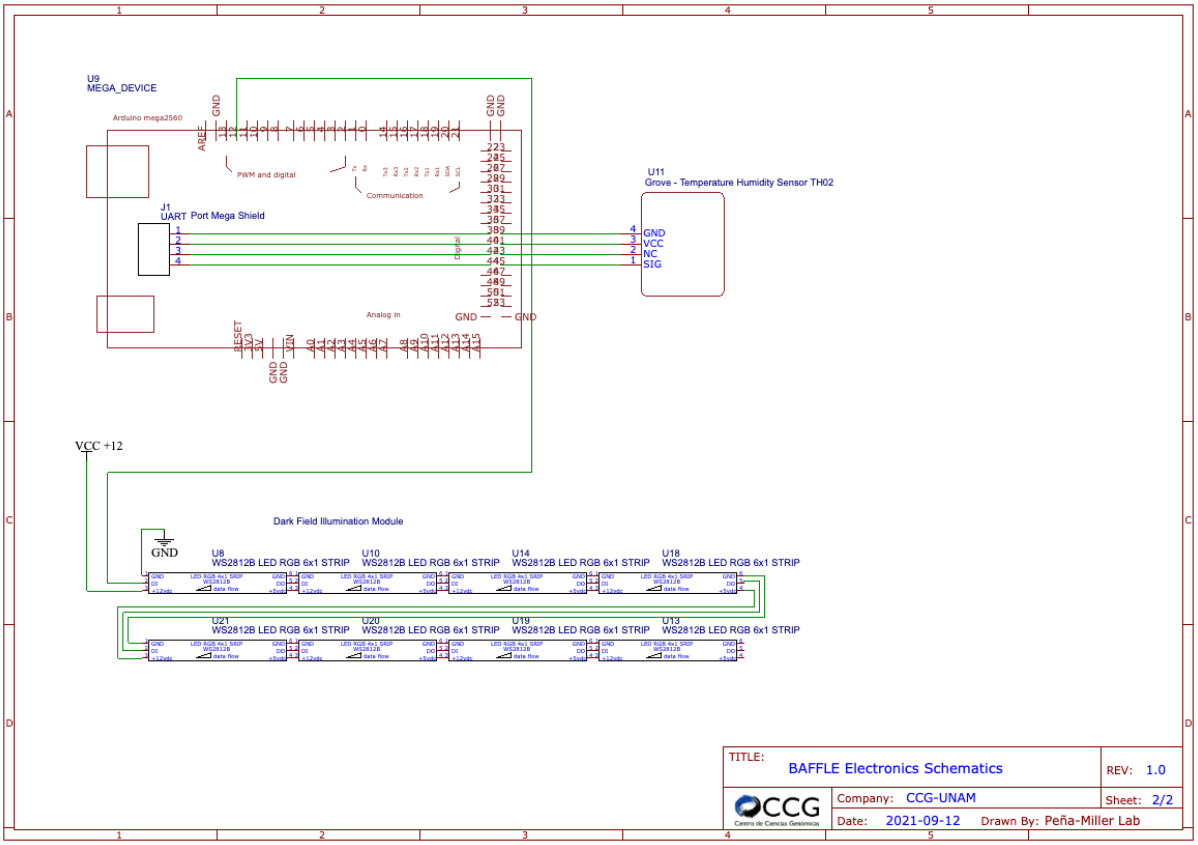

Figure 11: Electronic schematics of the humidity and temperature sensors, and dark field illumination module.

Strain	*Phenotype*	*Fluorescence*	*Experiment*	*Source*
Escherichia coli BW25113	Wild-Type	No	Calibration	[3]
E. coli MG1655-Crimson	Plasmid encoding E2Crimson protein	Red	Calibration	[4]
E. coli MG1655-DsRed	Plasmid encoding DsRed protein	Red	Calibration	[4]
E. coli MG1655-GFPmut3	Plasmid encoding GFPmut3 protein	Green	Calibration	[4]
E. coli MG1655-mVenus	Plasmid encoding mVenus protein	Yellow	Calibration	[4]
E. coli MG1655-Cyan	Plasmid encoding sCFPA3 protein	Cyan	Calibration	[4]
E. coli tyrA-	Tyrosine auxotrophy	No	Colony counts	[3]
E. coli tyrA-pBGT-1	Tyrosine auxotrophy encoding TEM-1 β-lactamase	Green	Colony counts	[3, 36]
E. coli Gby	Kanamycin resistance & YFP protein	Yellow	Gradient	[10, 11]
E. coli Wcl	Kanamycin susceptible & CFP protein	Cyan	Gradient	[10, 11]
E. coli-mCherry	MG1655 and mCherry protein	Red	Expansion	This study
E. coli pBGT-1	Mg1655 with pBGT-1 plasmid	Green	Expansion	[36]
Paenibacillus lautus	Pattern forming	No	Expansion	F. Federici
Paenibacillus dendritiformis	T morphotype 30A1	No	Morphology	Bacillus Stock Center (OSU)

Table 2: Strains used in the experiments presented in this study.